



ARTICLE

Perceiving the Trend of Terrestrial Climate Change during the Past 40 year (1978-2018)

Asheesh Bhargawa* A. K. Singh

Physics Department, University of Lucknow, Lucknow-226 007, India

ARTICLE INFO

Article history

Received: 21 October 2020

Accepted: 16 November 2020

Published Online: 31 January 2021

Keywords:

Principal component analysis

Total solar irradiance (TSI)

Cloud cover

CO₂ abundance

Global surface temperature (GST) anomaly

Global climate index (GCI)

ABSTRACT

In past few decades, climate has manifested numerous shifts in its trend. Various natural and anthropogenic factors have influenced the dynamics and the trends of climate change at longer time scale. To understand the long term climate fluctuations, we have analyzed forty years (1978 - 2018) data of ten climatic parameters that are responsible to influence the climate dynamics. The parameters involved in the present study are total solar irradiance (TSI), ultra violet (UV) index, cloud cover, carbon dioxide (CO₂) abundances, multivariate (ENSO) index, volcanic explosivity index (VEI), global surface temperature (GST) anomaly, global sea ice extent, global mean sea level and global precipitation anomaly. Using the above mentioned climate entities; we have constructed a proxy index to study the quantitative measure of the climate change. In this process these indicators were aggregated to a single proxy index as global climate index (GCI) that has measured the strength of present climate change in semblance with the past natural variability. To construct GCI, the principal component analysis (PCA) has been used on yearly based data for the period 1978 - 2018. Actually PCA is a statistical tool with which we can reduce the dimensionality of the data and it retains most of the variation in the new data set. Further, we have confined our study to natural climate drivers and anthropogenic climate drivers. Our result has indicated that the strongest climate change has been occurred globally by the end of the year 2018 in comparison to late 1970's natural variability.

1. Introduction

In our daily life generally we deal with the term like weather, which includes the short term perspective of the circumstances of temperature, humidity, cloud cover, wind and rain. The Climate is the long-term concept which is defined as the weather conditions prevailing for a large time span in an area and is predominantly determined by

temperature and precipitation of that particular area^[1]. The flora and fauna found in a particular region is largely determined by the climatic conditions found there^[2]. This shows the importance of crucial role played by climate in ecology and human life. Climate shows its variability in form of seasonal cycles or cyclic variations which may include the time span from a year to several years or even decades, such as the great Indian monsoon, North Atlantic

**Corresponding Author:*

Asheesh Bhargawa,

Physics Department, University of Lucknow, Lucknow-226 007, India;

Email: asheeshbhargawa@gmail.com

oscillations (NAO), El Niño events etc.

Solar radiation reaching Earth's surface in the main driver of long term climate change as its intensity and distribution may change over various time scales^[3,4]. The solar brightness fluctuates continuously with a noticeable 11-year cycle is now unambiguous, as an outcome of direct observations of solar irradiance recorded by various space-based radiometers since late 1978^[5]. The climate system of our planet shows an evident response to solar variability, other natural forcings and anthropogenic influences on various time scales. Generally we observe the magnitude of these responses quantified in parameters such as global mean surface temperatures and global sea surface temperature^[6]. In recent past the interaction between the human beings and the nature became very disastrous^[7]. As a consequence of these anthropogenic disturbances the Earth's climate is undergoing substantial and rapid changes^[8].

Our ability to understand and model the physical drivers of climate change have been increased based on the past observation of patterns and trend shown by terrestrial climate. With the model studies we can understand the causes of past and present climate change and can predict the future changes directly^[9,10]. The interconnectedness and complexity of the components of the climate system such as the land, ocean, atmosphere and cryosphere, have posed some challenges in front of us. It has long been predicted that the increased global warming is directly associated with the increasing amount of greenhouse gases in the atmosphere^[11]. According to Xia et al.,^[12] the global mean surface temperature has increased with a rate less than 0.1°C /decade in the past century. During the past decades of 1980s and 1990s several times we have achieved the record global temperatures, but a new height of temperature often surpasses the old one by only a few amount of a degree.

The approaches for perceiving climate change generally involve the estimation of the time series models which involve the relation between relevant forcing variables and climatic parameters^[13,14]. The credibility of the models use for climate studies depends significantly on the time series properties of both the forcing and response variables^[15]. Generally, the time series representing various forcings of climate dynamics show a non-stationary and stochastically behaviour^[16]; for this reason we have to rely only on the changes in the response variables because they are stationary in nature which undermines the trustworthiness of application of classical models which generally follow the static regression analysis^[17].

At present the scientific activity related to climate studies have mostly been oriented towards the development of techniques with which they may be able to detect a significant climate change mathematically. But the condition is that, these calculations must involve the natural and anthropogenic climate forcings^[18]. As the observed climate change is an overall response of not only of natural and man-made forcings, such as solar irradiance changes and increasing greenhouse gases, but it also includes the chaotic or unforced variability of the climate system like volcanic eruptions and El Niños^[7,19]. This makes the detection of climate change a tough job.

To address this credibility issue related to climate change we have analysed all possible mechanisms of the climate dynamics in an inclusive manner. To that end we have tried to propose a proxy climate index representing the intended assessment of practical climate change mathematically. This index is a composite of some climate factors (natural and anthropogenic) and indicators, such as Total solar irradiance, global surface temperature anomaly, increasing greenhouse effect etc. Our climate index deal in a multi-dimensional approach that is, we have included all the major forcings which directly or indirectly affect the climate of the Earth. We also compared recent observed climate change with the climatic conditions which occurred in the 1970s. Finally, we examine recent growth rates of global surface temperature, greenhouse gases and have tried to assess the present global warming. The main objective of this study is to construct an index of climate change and to explore the temporal variability of the climate system on the globe. Our focus is to explore the climatic variables and the climatic factors (structure) which may influence in the climate change globally.

To find the Global Climate Index (GCI), which is a proxy parameter for climate change, we have used Principle component analysis (PCA) method. The principal component analysis (PCA) is a mathematical tool with which we can reduce the dimensionality of a given data set having a vast number of interrelated variables, while retaining the maximum possible variation present in the data set concerned^[20]. For this a new set of variables needs to be created known as the principal components (PCs), which must not correlated to each other, and are well-organized so that the first few preserve most of the variation which were present in all of the previous input variables^[21].

This paper is organized in various sections. As customary, section 1 has presented the brief introduction. Section 2 has described data and methodology used to evaluate the

global climate index. Section 3 has presented the details of basic parameters of climate and various climate indicators. Section 4 has presented the calculation of the global climate index. Results and discussion are presented in section 5. Finally, section 6 has presented the conclusion.

2. Data and Methodology

We have collected a total of ten time series data for the present analysis. We have adopted the way to select our time series parameters according to climate forcings or climate drivers. Firstly we considered the natural climate drivers, which included changes in the sun's energy output (total solar irradiance), UV index, cloud cover variations, multivariate ENSO index and large volcanic eruptions (that throw a huge number of particles into the upper atmosphere that reflect sun light). Further the anthropogenic climate drivers, which included emissions of heat trapping gases. The climate data used to compute our index is obtained from different viable sources which are given in the following subsection.

2.1 Data Sources

The last 40 year (1978-2018) data of climatic factors and indicators were used to compute global climate index. The total solar irradiance data are taken from the website of Laboratory for Atmospheric and Space Physics (LASP) of University of Colorado Boulder data base (<http://lasp.colorado.edu>) while UV index data was taken from NEO NASA Earth observation (<https://neo.sci.gsfc.nasa.gov/>). The cloud cover data was taken from the International Satellite Cloud Climatology Project (ISCCP) (<http://isccp.giss.nasa.gov/>). Data for the MEI is published by ESRL physical division (<https://www.esrl.noaa.gov/>). Data for volcanic eruptions, particular for the periods of eruption, was sourced from the Smithsonian Institution (<http://volcano.si.edu/>), Under Global Volcanism Program and the data of CO₂ is obtained from NOAA Earth System Research Laboratory (<https://www.esrl.noaa.gov/gmd/>) and the data of CO₂ is obtained from NOAA Earth System Research Laboratory (<https://www.esrl.noaa.gov/gmd/>). The global surface temperature anomaly data was obtained from the Earth Sciences Division, Goddard Institute for Space Studies (GISS), NASA (<https://data.giss.nasa.gov/gistemp/>). The global Sea Ice Extent data are obtained from NOAA's National centre for environmental Information (NCEI) website (<https://www.ncdc.noaa.gov/>). The global Mean Sea Level Data is obtained from Physical Oceanography Distributed Active Archive Centre (<ftp://podaac.jpl.nasa.gov>). The global precipitation anomaly data is

obtained from Environmental Protection Agency, USA (www.epa.gov).

2.2 Principal Component Analysis

The Principal component analysis (PCA) is a mathematical technique which reduces the number of variables in a given data set into a lesser number of dimensions as comparison to the input data. This can be understood in mathematical terms as - suppose we an initial set of n correlated variables say variables X_1 through to X_n , then by using PCA we can create a new set of uncorrelated components or indices known as principle components, where each component in new data set will be a linear weighted combination of the input variables. Therefore the principle components can be written as -

$$\begin{aligned} PC_1 &= a_{11}X_1 + a_{12}X_2 + \dots + a_{1n}X_n \\ PC_m &= a_{m1}X_1 + a_{m2}X_2 + \dots + a_{mn}X_n \end{aligned} \quad (1)$$

Where a_{mn} is a manifestation of the weight for the m^{th} principal component (PC_m) and the n^{th} variable.

The weights for each principal component (PCs) can be calculated by the eigenvectors of the correlation matrix or the co-variance matrix (in case the original data were standardized). The variance for each principal component (PCs) can be found by the eigenvalue of the corresponding eigenvector. The components are organised so that the first component (PC_1) shows the largest possible amount of variation in the input data. The second component (PC_2) must be completely uncorrelated with the first component (PC_1), and explains second maximum variation, subject to the same calculation. Succeeding components must also show an uncorrelation with previously calculated components i.e. PC_1 and PC_2 ; therefore, each subsequent principle component captures an additional dimension in the data, while explaining smaller and smaller proportions of the variation of the original variables. An extensive description of PCA can be found in ^[21], and its applications to related to climate studies are given in ^[22].

3. Parametric Selection for calculation of Global Climate Index (GCI)

Solar activity variations, in particular the solar electromagnetic radiation indeed affects the Earth's climate on long run. On the other hand in recent past the anthropogenic factor has also become an important player in climate change. Further the natural forcing including internal climate factors, such as volcanoes and El Niño changes in climate patterns leading to changes in the various dimensions of climate dynamics ^[23]. A schematic view of differ-

ent forces affecting climate is presented in Figure 1.

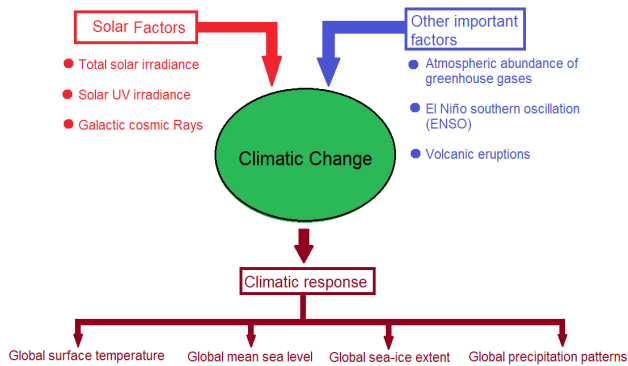


Figure 1. A scheme of the climate forcing

3.1 Parameters related to Solar Forcing

Three principal mechanisms have been known that provide a link between the solar variability and respective changes occurred into the Earth's climate conditions. The first mechanism, originally proposed by Herschel^[24], is about the changes in *total solar irradiance (TSI)* measurements which discusses a variable heat input (mostly in visible and infrared wavelengths) to the troposphere^[25,26]. The second suggested forcing mechanism is about variation in *solar ultraviolet radiation* especially during the solar cycle. This hypothesis is based on the fact that changes in the ozone concentrations may results into the heating of the stratosphere, where the ultraviolet radiation is absorbed^[27,28]. The third suggested forcing mechanism is through the effect of galactic cosmic rays on the weather and climate^[29], involves *cloud processes* such as condensation nucleus abundances^[30], thunderstorm electrification and thermodynamics^[31], or ice formation in cyclones^[32].

3.1.1 Total Solar Irradiance

Figure 2(a) shows the total solar irradiance (TSI) monthly variations. The TSI is a measure of the integrated solar energy flux over the entire spectrum arriving at the top of the terrestrial atmosphere at the mean Sun-Earth distance and have a potential to cause long time climate change^[33]. Measurements show that over the time span of 11 year (one solar cycle), the solar radiation energy fluctuates on average at about 0.1 %. The Sun emits a huge amount of radiative energy (about 1,361 watts per square meter), even this small change in solar output energy can affect terrestrial climate^[14]. This fluctuations in the solar radiation occurred during a solar cycle may impact surface temperature by about 0.1 degree Celsius globally^[26].

Camp and Tung^[34] have observed a variation in the surface air temperature which is about $(0.18 \pm 0.10 \text{ }^\circ\text{C})$ from solar minimum to maximum during the solar cycles from 1959 to 2004.

3.1.2 Solar UV Index

Figure 2 (b) depicts the variations in UV index which is a measurement of ultraviolet (UV) radiation reaching at surface of the Earth. The thickness of stratospheric ozone is the main parameter that determines the intensity of surface UV radiation in the clear sky conditions. The reduction of 1% in stratospheric ozone column may results into the enhancement of surface UV radiation by 1.1% in absence of clouds^[35]. At present the main concern of UV enhancement at the surface is due to ozone depletion in the stratosphere. This depletion has been occurred mainly because of the increasing amounts of atmospheric chlorine and bromine that have been predominantly originated from the photo dissociation of chlorofluorocarbon compounds (CFCs) emitted at the surface^[36].

The ground-level strength of solar ultraviolet (UV) radiation i.e., UV index can be used to measure and forecast the level of stratospheric ozone concentration^[37]. From late 1970's a negative trend in total ozone column amount has been witnessed globally which makes a great concern for the climate change studies. Since stratospheric ozone absorbs the solar ultraviolet (UV) directly incident on it, the decrease in its amount may be responsible for the enhancement of UV irradiance in the troposphere down to the surface^[11,38]. Therefore changes in stratospheric ozone can impact climate because the changes in stratospheric ozone may bring changes in the large scale atmospheric state such as tropospheric circulation, surface weather and the amount of surface UV radiation^[38].

3.1.3 Cloud Cover Variation

One of the most important indirect forcing that might have potential to influence the terrestrial climate is variation in cloud cover through cosmic rays. As we know the cloud cover obstructs the flow of solar radiation, which directly implies that the clouds can control the incident amount of solar radiation reaching the surface of the Earth during the day time, and it also controls the amount of heat that lost during overnight that is cooling of near surface environment^[39-41]. Sunspots are the indicators of state of the solar magnetic activity and therefore they also represent the amount of solar modulation of galactic cosmic rays, and hence their intensity at the Earth^[42]. The hypothesis that links the cosmic ray and climate is about an

ionization event by a cosmic ray that produces a charged aerosol particle and boosts its capacity to nucleate a droplet and contribute to its subsequent growth. As a result of this water vapour condenses on these particles leading to formation of clouds. Thus during a solar maximum there is a decreased in intensity of cosmic rays implies lesser clouds and hence higher surface temperature^[43]. The percent variation in cloud cover from 1978 to 2018 has been shown in the figure 2 (c).

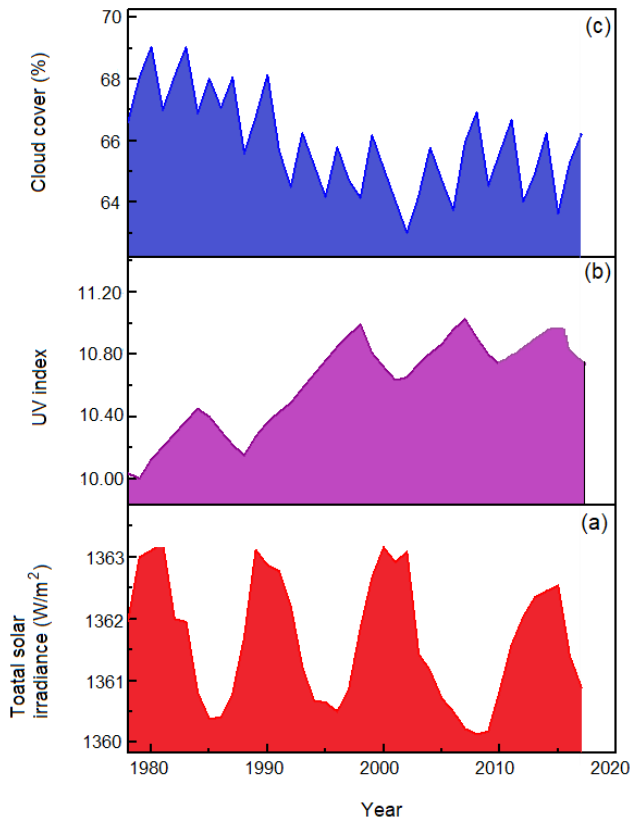


Figure 2. Monthly average variations of (a) total solar irradiance, (b) UV index and (c) cloud cover for the period 1978-2018

3.2 Parameters Related to Other Important Drivers

There are other three major drivers of climate which play an important role in the climate dynamic, which is greenhouse gas effect, volcanic activity and El Niño southern oscillation (ENSO). In this study atmospheric abundance of CO₂, Multivariate ENSO index (MEI) and Volcanic Explosivity Index (VEI) has been taken as the representative parameters of above climatic drivers.

3.2.1 Atmospheric Abundance of CO₂

Since mid of 20th century the amount of greenhouse

gases has been increased rapidly from human activities are this is the foremost substantial driver of observed climate change^[44]. The anthropogenic activities are solely responsible for an increase of 35 % in the net amounts of greenhouse gases since 1970's whereas the emission of carbon dioxide, which account for about 75% of total emissions, have been increased by 42 % over this same period^[14]. The first panel of Figure 3(a) shows the global atmospheric abundance of CO₂ from the year 1978 to 2018. From figure we can observe that global atmospheric concentrations of carbon dioxide have risen significantly over the last few decades. Around 1978 this abundance was about 335.37 ppm (parts per million) while during 1990 it was 353.98 ppm and during the year 2000 it was 369.06 ppm. The current atmospheric abundance is about 408.61 ppm. Based on the above results we have observed the rate of increase in atmospheric abundance of CO₂ is about 18.31 ppm per decade.

3.2.2 Multivariate ENSO Index (MEI)

The complex system of ocean currents may also have a significant impact over the climate system of the Earth^[45]. These effects are in the form of fluctuations or oscillations in the water conveying belts of the oceanic water and the El Niño and La Niña are two best-known oscillations of that kind^[46]. The La Niña is the opposite of the El Niño condition and these two collectively make up an oscillation termed as El Niño southern oscillation (ENSO). Figure 3(b) shows the multivariate ENSO index (MEI) variation, which directly relates the El Niño (warm phase) and La Niña (cold phase). The fluctuations in ENSO index have directly been associated with irregular climatic patterns and these oscillations are the largest source of inter-annual climate variability, contributing to substantial changes in temperature, rainfall, and extreme weather conditions globally^[47-49].

3.2.3 Volcanic Explosivity Index (VEI)

Figure 3(c) shows the total Volcanic Explosivity Index (VEI) for the year 1978 to 2018 which indicates the intensity of volcanic explosions. The gases and dust particles flung into the near surface atmosphere during volcanic eruptions have a significant impact on climate^[50]. These elements ejected from volcanoes have a cooling effect in the planet by shielding the incoming radiation from the Sun^[16]. This cooling effect may last for a long period of time ranging from months to years depending on the intensity of the eruption^[15,51,52].

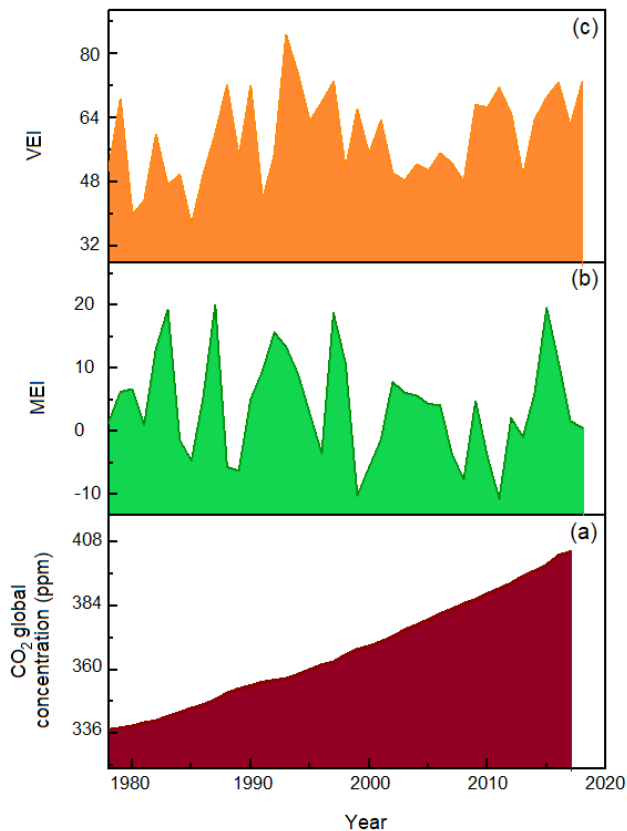


Figure 3. Variation of atmospheric burden of (a) CO₂, (b) the MEI and (c) the VEI for the period 1978 to 2018

3.3 Determinates of the Climate Change

These are the set of parameters that label the various aspects of changing climate of the Earth. They indicate the key features for the most relevant realms of climate change such as temperatures, ocean, atmosphere and the cryosphere.

3.3.1 Global Surface Temperature Anomaly

Global surface temperature anomaly is measure of overall average surface temperature of the Earth that deviates from expected value based on past measurements^[53]. The warmer temperature than a reference value will have a positive anomaly while negative anomaly means a cooler temperature than that of the reference value^[3]. Figure 4 (a) has showed the variation in global temperature anomaly for the period 1978 to 2018. As we can see from the figure, in year 1978 (starting year of analysis) the observed value of the surface temperature anomaly was about 0.13⁰C. Further an increasing trend was observed during the 80's period. Here the anomaly in temperature rose up to the value of 0.41⁰C. In the year 1990 the global temperature anomaly reached at value of 0.37⁰C and after

on decade it reached at the value of 0.56⁰C. The global temperature anomalies for the year 2010 and 2018 are as 0.71⁰C and 0.99⁰C respectively^[54,55].

3.3.2 Global Mean Sea Level

Sea level has shown a continuously rising trend over the past few decades. During the year 1993 the highest annual average in sea level was recorded. This was the highest level till that period but in 2017, global mean sea level was observed to be 3 inches above the value of 1993 average. The variation in the global mean sea level (GMSL) is shown in second panel of Figure 4(b). We can see a continuous increase in the sea levels from 1993 to present time. This rapid change in GMSL is indicating that the climate of our planet is undergoing a change. The main reason for the increase in global-mean sea level rise is the global warming^[56]. As a result of global warming the ice sheets and glaciers are melting and they are adding more water to the oceans^[1,14,57].

3.3.3 Global Sea-ice Extent

The global sea ice extent has made concerns in the scientific community because of its rapidly decreasing amount especially in the Arctic region^[58-60]. This decrease in sea ice is an important indicator of global climate change^[10,18]. The present global warming is also transferring heat to oceans, resulting in further ice reductions^[61]. The sea ice in the Antarctic region particularly in the Southern Ocean surrounding Antarctica has also received attention because the sea ice coverage there, has increased rather than decreased since the late 1970s^[17,62]. But these sea ice increases observed in the Antarctic region have not been as large as the sea ice decreases observed in the Arctic region^[63]. Figure 4(c) shows that the present status of sea ice extent is about 24.3 million sq. km. The rate of reduction of the global ice extent is about 0.06 million sq. km/year^[18,64].

3.3.4 Global Precipitation Anomaly

The fourth panel of Figure 4 (d) shows the global precipitation anomaly. As figure shows, the global annual precipitation has undergone a significant inter-annual variability especially during past few decades. Based on the moving averages it can be seen that precipitation anomaly was lower than 1 mm from 1979 up until around 1981. Between 1986 and 1990 the precipitation was approximately -2 mm. The total annual precipitation has increased over land globally. Since 1978, global precipitation has increased at an average rate of 0.08 inches per decade. Zhang et al.,^[65] have observed the precipitation anomaly

from 1998 to 2015 and have concluded that average annual precipitation anomaly values are less than the previous one.

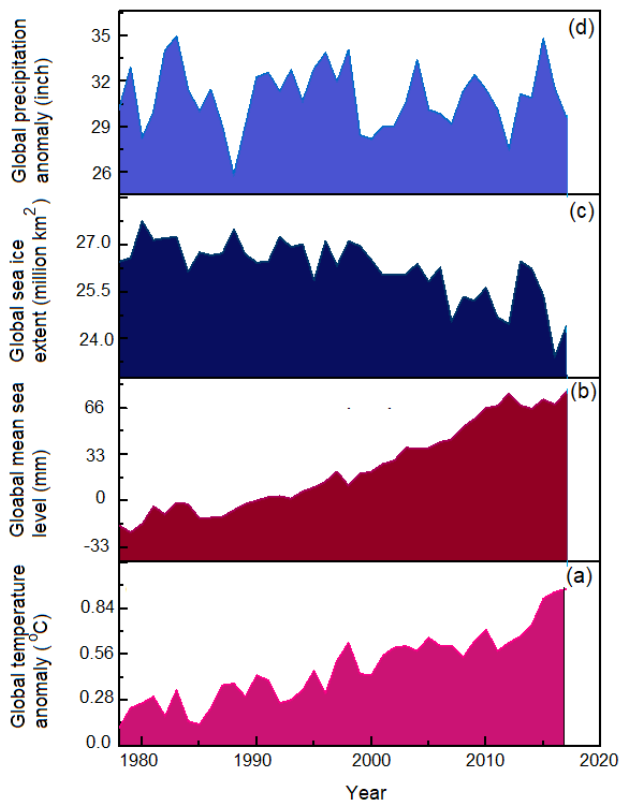


Figure 4. Temporal variation of some climate indicators namely (a) global surface temperature anomaly, (b) Global mean sea level, (c) global sea ice extent and (d) global precipitation anomaly for the period 1978-2018

4. Calculation of Global Climate Index (GCI)

The composite index, named global climate index (GCI) based on the time series data from 1978 to 2018, was developed by using principal component analysis (PCA). For this we have selected 10 climatic entities. The index relates to the climatic conditions globally. It is derived from attributes such as solar irradiance, atmospheric abundance of CO₂ and Global surface temperature anomaly. Various solar, natural, and anthropogenic variables were included to ensure a multidimensional approach in understanding trends of climate change. The variables that are employed in global climate index construction are: solar irradiance, UV index, cloud cover variation, MEI, VEI, CO₂ abundance, global surface temperature anomaly, global mean sea level, global sea ice extent and global precipitation anomaly.

Table 1 gives a summary of all the time series data

used in the construction of GCI. It contains the minimum, maximum, Mean and standard deviation of each time series of parameters. With the help of these ten variables (let's say; X₁, X₂,...,X₁₀) we have calculated the correlation matrix which is shown in Table 2. This table simply gives the coefficients of correlation (σ) between each of the 10 variables. The high degree of inter-correlation between the physical variables is evident from this table. There are a number of interesting observations which may be made by inspection of these correlations. Atmospheric abundance of CO₂, Global surface temperature anomaly and Global mean sea level were well correlated with UV index (Correlation coefficient $\sigma = 0.897$, $\sigma = 0.835$ and $\sigma = 0.863$ respectively). Whereas the cloud cover and global sea ice extent have a noticeable anti-correlation with UV index ($\sigma = -0.611$ and $\sigma = -0.622$). Cloud cover have a significant anti-correlation with CO₂ abundance, Global surface temperature anomaly and Global mean sea level ($\sigma = -0.563$, $\sigma = -0.553$ and $\sigma = -0.520$). MEI showed a good correlation with global precipitation anomaly ($\sigma = 0.503$). Atmospheric abundance of CO₂ is highly correlated with Global surface temperature anomaly and Global mean sea level ($\sigma = 0.928$, $\sigma = 0.980$) but it has a high level of anti-correlation with Global sea ice extent ($\sigma = -0.763$). Global surface temperature anomaly showed a good correlation with Global mean sea level and has a significant anti correlation with Global sea ice extent ($\sigma = 0.897$, $\sigma = -0.711$). Global mean sea level have highly anti correlated with Global sea ice extent ($\sigma = -0.77$).

Further we have calculated the eigenvalues of the correlation matrix, and the corresponding ten eigenvalues are given in Table 3. Table also gives the recent variance of each principal component related to a particular eigenvalue (Figure 5). From the figure 5 we can observe that the first principle component shows 48.5 % variability for the considered climate system, and the second component shows variability equal to 15.9 %. Similarly we can get the variability of each successive principle component as we proceed downward in the third column of the table. It is necessary to decide on the number of components which have any practical significance. A simpler but arbitrary rule of thumb, which has proved to be useful in practice, is to consider only those components which have eigenvalues of 1.0 or greater as having any practical significance. In this study, therefore, the first three components, accounting for about 75% of the total variability, would be regarded as being of practical significance, although the possible interpretation of the next two components, bringing the total variability to about 90.5%, would also be considered.

Table 1. Summary of the parameters used in the calculation of Global Climate Index (GCI)

Variable symbol	Variable	Minimum	Mean	maximum	Standard deviation
X ₁	Solar irradiance	1360.53	1361.10	1361.68	0.37
X ₂	UV index	9.88	10.71	11.37	0.43
X ₃	Cloud cover	63.65	66.38	69.38	1.47
X ₄	MEI	-10.71	4.10	19.97	8.25
X ₅	VEI	37.42	58.78	84.76	10.99
X ₆	CO ₂ abundance	337.40	366.78	404.30	20.24
X ₇	Global surface temperature anomaly	0.11	0.47	0.96	0.21
X ₈	Global mean sea level	-22.5	22.72	77.30	30.94
X ₉	Global sea ice extent	23.43	26.23	27.75	0.94
X ₁₀	Global precipitation anomaly	25.9	30.88	34.76	2.00

Table 2. Correlation matrix for all the ten parameters used in the analysis

	Solar irradiance	UV index	Cloud cover	MEI	VEI	CO ₂ abundance	Global surface temperature anomaly	Global mean sea level	Global sea ice extent	Global precipitation anomaly
Solar irradiance	1	-0.314	0.068	0.038	-0.097	-0.198	-0.099	-0.189	0.295	-0.154
UV index	-0.314	1	-0.611	-0.050	0.242	0.897	0.835	0.863	-0.622	0.130
Cloud cover	0.068	-0.611	1	-0.028	-0.195	-0.563	-0.553	-0.520	0.33	0.076
MEI	0.038	-0.050	-0.028	1	0.107	-0.146	0.040	-0.160	0.161	0.503
VEI	-0.097	0.242	-0.195	0.107	1	0.272	0.252	0.237	-0.235	0.096
CO₂ abundance	-0.198	0.897	-0.563	-0.146	0.272	1	0.928	0.980	-0.763	-0.048
Global surface temperature anomaly	-0.099	0.835	-0.553	0.040	0.252	0.928	1	0.897	-0.711	0.008
Global mean sea level	-0.189	0.863	-0.520	-0.160	0.237	0.980	0.897	1	-0.77	-0.032
Global sea ice extent	0.295	-0.622	0.33	0.161	-0.235	-0.763	-0.711	-0.77	1	0.071
Global precipitation anomaly	-0.154	0.130	0.076	0.503	0.096	-0.048	0.008	-0.032	0.071	1

Table 3. Eigen values corresponding to each parameter and their percentage variability

Component	Eigenvalues	Percentage of variability	
		Component	Cumulative
PC ₁	4.854	48.5	48.5
PC ₂	1.589	15.9	64.4
PC ₃	1.049	10.5	74.9
PC ₄	0.875	8.7	83.6
PC ₅	0.680	6.8	90.5
PC ₆	0.477	4.7	95.2
PC ₇	0.289	2.8	98.1
PC ₈	0.093	0.9	99.1
PC ₉	0.077	0.7	99.8
PC ₁₀	0.011	0.1	100

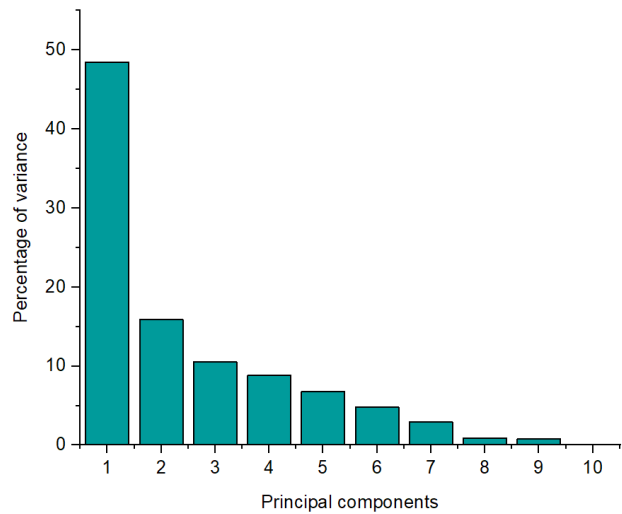


Figure 5. Percent variation of principal components

The results of PCA are presented in Table 4. Five factors accounted for 90 per cent of the total variance in the data. For the first factor (PC₁) the global surface temperature anomaly showed markedly higher positive loading which is equal to 0.9730. Here loading are correlation coefficients of each variable with the factor, so they natu-

Table 4. Result of principal component analysis

Variables	PC 1	PC 2	PC 3	PC 4	PC 5	PC 6	PC 7	PC 8	PC 9	PC 10
Solar irradiance	-0.1266	0.0077	0.9211	-0.0208	0.3789	0.1807	-0.3503	0.0068	-0.1463	0.1966
UV index	0.2181	-0.1216	-0.0365	-0.1312	-0.1101	0.7527	0.0893	-0.221	0.3098	0.2455
Cloud cover	-0.292	0.0057	-0.3274	0.0344	0.7831	0.1227	-0.019	-0.0409	0.4074	-0.0991
MEI	-0.0468	0.022	0.0707	-0.1133	-0.0501	0.1349	0.7616	0.1644	0.1413	-0.6369
VEI	0.1511	-0.0278	0.06	0.8515	0.0307	0.0028	0.2344	-0.01	0.0495	0.0943
CO ₂ abundance	0.4439	0.9161	0.0416	-0.1509	0.116	-0.1149	-0.053	0.2555	0.1894	0.0417
Global surface temperature anomaly	0.9730	-0.1718	0.1783	-0.1023	0.1526	-0.4894	0.0439	-0.6497	0.2145	-0.1331
Global mean sea level	0.4353	-0.5357	0.0209	-0.0812	0.1801	-0.1862	-0.0616	0.6527	0.1288	0.0522
Global sea ice extent	-0.367	-0.0059	0.1966	-0.0365	-0.3335	-0.2384	0.0867	0.0913	0.5129	0.3644
Global precipitation anomaly	-0.004	0.033	-0.132	-0.2048	0.2169	-0.1519	0.4784	-0.0177	-0.2953	0.567

rally range from -1 to +1.

A negative loading simply means that the results need to be interpreted in the opposite direction from the way it is worded. Loadings (linear weights) acquired through PCA from the reference data (Table 4) can be used as coefficients that define new climate indices. The values of the eigenvectors of these all the components are given in Table 4, the vectors being scaled so that the maximum weighting is + 1. Interpretation of the weightings may then be attempted fairly simply, by considering those variables which have relatively high positive or negative weighting (> 0.7) as constituting the global climate index (GCI) which is combined action of the original considered variables.

The second principle component (PC₂), giving relatively high positive weighting to the atmospheric abundance of CO₂ may be regarded as a general constituents of the anthropogenic climate change. From the table we can observe that the correlation between PC₂ and atmospheric abundance of CO₂ is equal to 0.9161. This simply indicates that the second principle component is a measure of anthropogenic contribution in the climate system. The third principle component (PC₃) is a measure of the influence of solar irradiance variability on the climate dynamics because it shows high correlation with total solar irradiance (viz. 0.9211). The fourth principle component (PC₄) is a contribution of mainly VEI as it shows highest loading (correlation) with VEI which is equal to 0.8515. The fifth principle component can be directly associated with measure of cloud cover. The correlation coefficient between PC₅ and cloud cover is about 0.7831. The sixth principle component (PC₆) has highest loading of UV index (about 0.7527). Therefore it is a measure of influence of UV index on climate dynamics. The seventh principle component (PC₇) can be considered as a measure of cloud MEI effects on climate system. It has a highest correlation value about 0.7616 with MEI. The rest of principle components that is PC₈, PC₉ and PC₁₀ showed lower correlation with global mean sea level, global sea ice extent and global precipitation anomaly respectively. As seen from the table 4 the values of these correlation coefficients are 0.6527, 0.5129 and 0.567 respectively.

Next step is to obtain principal components using eigenvectors (Loadings) of the estimated correlation matrix. The principal components will be obtained by using the formula given in equation (1). Therefor the first principal component can be written as;

$$PC_1 = (-0.1266) X_1 + (0.2181) X_2 + (-0.2920) X_3 + (-0.0468) X_4 + (0.1511) X_5 + (0.4439) X_6 + (0.9730) X_7 + (0.4353) X_8 + (-0.3670) X_9 + (-0.0040) X_{10}$$

Using above equation we have calculate all the data

points of first principal component (PC₁). From the table 3 we have seen that this principle component (PC) shows maximum variability of the climate system concerned in the analysis (48.5 %) and it is highly correlated with global surface temperature (GST) anomaly. Figure 6 depicts the correlation between PC₁ and GST anomaly. Because of this high degree of variability and correlation with GST anomaly, the PC₁ can be taken as a proxy index representing the global warming of the planet Earth. Therefore in this study the first PC has been considered as GCI which represents total warming and cooling patterns caused by both the natural as well as anthropogenic factors. The obtained time series of PC₁ has been plotted in figure 8 (blue line).

The Second principal component (PC₂) shows a high degree of correlation with CO₂ abundance (figure 7) and it has second maximum variably for the climate system (15.9 %). Therefore this PC gives a measure of human induced warming in the terrestrial climate excluding natural factors. Figure 8 (red line) shows the warming pattern due to increase in atmospheric abundance of greenhouse gases predominantly CO₂. The Second principal component can be calculated as;

$$PC_2 = (0.0077) X_1 + (-0.1216) X_2 + (0.0057) X_3 + (0.022) X_4 + (-0.0278) X_5 + (0.9161) X_6 + (-0.1718) X_7 + (-0.5357) X_8 + (-0.0059) X_9 + (0.033) X_{10}$$

As discussed above the principle components PC₃, PC₄, PC₅, PC₆ and PC₇ showed high degree of correlation with natural factors of climate dynamics e.g. TSI, VEI, cloud cover, UV index and MEI respectively, but their variability of climate system decreases continuously as 10.5%, 08.7%, 6.8%, 4.7% and 2.8% respectively. Therefore we have calculated the overall impact of natural factors in climate system. For this we have constructed another proxy index containing the impact of all five principle components from PC₃ to PC₇. This proxy index denoted by PC_N is a measure of warning and cooling due to variation in natural factors excluding the anthropogenic factors. The composite index for natural forcing (PC_N) has been constructed using the obtained eigenvalues of variables and principal components as under:

$$PC_N = \frac{\lambda_3 PC_3 + \lambda_4 PC_4 + \lambda_5 PC_5 + \lambda_6 PC_6 + \lambda_7 PC_7}{\sum_{j=3}^7 \lambda_j} \quad (2)$$

Where, λ_j are eigenvalues and PC_j are the principle component. Figure 8 (green line) depicts the global warming due to variations in natural factors of climate system.

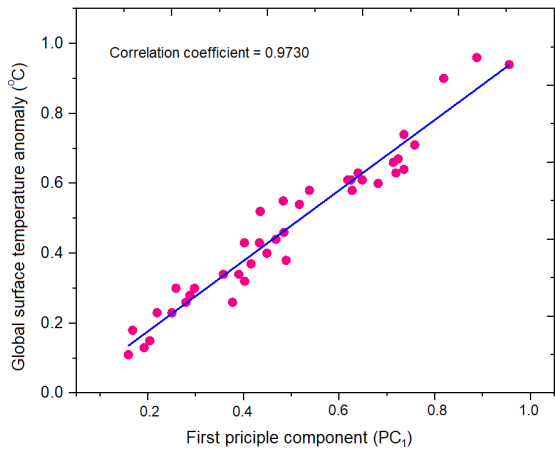


Figure 6. Correlation between First principle component (PC₁) and global surface temperature (GST) anomaly

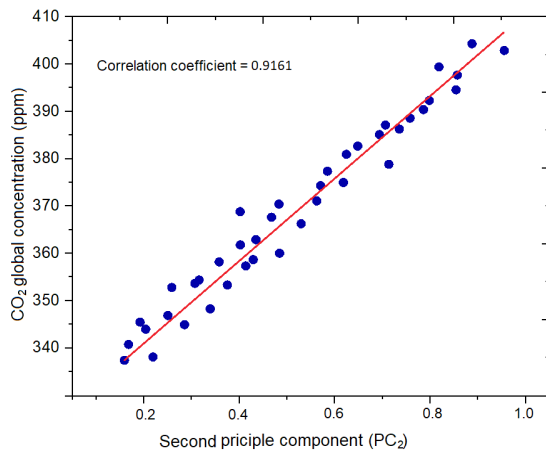


Figure 7. Correlation between second principle component (PC₂) and global concentrations of CO₂

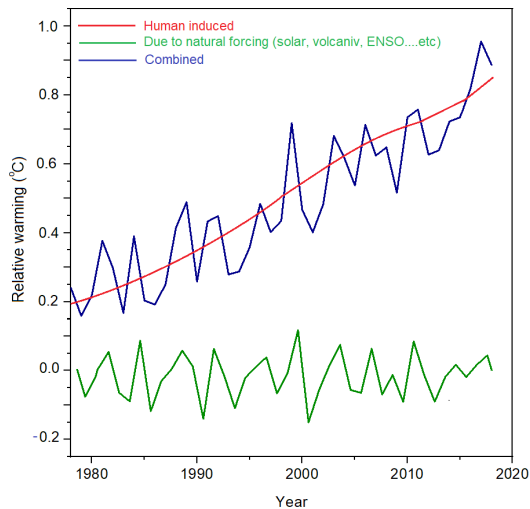


Figure 8. Global climate index (GCI) for the period from 1978 to 2018. The human -made contribution has shown in red. The natural contribution (solar, volcanic, ENSO,.. etc.) has depicted in green. The blue line shows the combined (total) temperature change driven by both natural and anthropogenic forcing

5. Results and Discussion

Climate change has been a challenging issue for the environmental scientists but at present it has been an issue for social, economic and scientific aspects as well. In the present paper, by using various involved parameters for climate change, we have generated a global climate index (GCI). To that end, we have analysed the time series data of all the considered climate parameters observed during last forty (1978-2018). Precisely we have selected total ten parameters and have developed an algorithm by using principal component analysis (PCA). Parameters involved are solar irradiance, UV index, cloud cover variations, MEI, VEI, CO₂ abundance, global mean sea level, global surface temperature anomaly, global precipitation anomaly and global sea ice extent. The positive values of global climate index (GCI) refer to changes in climate system that would be associated with warming patterns whereas the negative values would refer to the cooling trend. The discussed above the GCI is based on yearly observed values of the climate indicators and the factors that are responsible for the climate change significantly. Therefore the global climate index (GCI) is a direct measure of the degree of practical climate change that is occurring in form of warming and cooling. It also manifests natural climate variability, which shows the complexity involved in perceiving a change of climate conditions that are naturally chaotic in nature.

Figure 8 has showed the increasing trend in global climate index derived from our analysis. We have proposed a proxy global climate Index following the well-established principle component analysis. The human-induced warming in the year 1978 was calculated about 0.19 °C. Increasing in a continuous way it reaches about 0.82 °C in the year 2018. Therefore the human-induced warming in 2018 has been calculated relative to the base year 1978, reached +0.63 °C with an uncertainty of ±0.07 as shown in Figure 8 (red line). The changes associated with natural forcing are calculated as -0.04 ± 0.013 °C. The naturally driven changes are very small in comparison to the anthropogenic contribution (green line in Figure 8). Here we observed that basically all the witnessed warming since the year 1978 is human cause (red line). The rate of anthropogenic warming may actually be increased over the last 40 years and is presently at +0.16 °C/decade based on the 1978-2018 period. This clearly shows that the calculated index is very sensitive to the anthropogenic forcing and relatively less sensitive to natural factors on an inter-annual or even inter-decadal timescales.

Figure 8 (blue line) shows the warming/ cooling patterns due to combined effects of natural and anthropogen-

ic forcings. The index shown in blue depicts many deviations from its mean value because of natural inter annual climate variability.

The advantage of showing the global climate trends through global climate index is that only global surface temperature (GST) warming does give a holistic picture of global climate change because under transient climate change conditions the rate of warming of land is at least twice as fast as the warming rate observed in case of oceans. Therefore this may create an ambiguity in the climate related observations. Hence it is better to observe climate related warming / cooling with an index which is a composite of both the land and oceanic factors causing climate change.

6. Conclusions

Global climate change has already had observable effects on the environment. Effects that had predicted in the past would result from global climate change are showing their consequences as loss of sea ice, accelerated sea level rise and more intense heat waves resulting in warming of the globe. These have been caused by many natural factors, including changes in the Sun, volcanoes, and changed frequency of ENSO and CO₂ levels. In understanding global climate changes it is necessary to combine many dimensions, including solar forcing, natural drivers of climate and anthropogenic effects. By combining these three different approaches, we have able to build a clear picture of climate change that would not be possible if each was presented independently. Using principal component analysis, we have computed a composite of different climate elements as well as measures of variability and climate change.

In the present study, we have generated a method to calculate the global climate index (GCI). The GCI is a measure for how strongly present climate is changing relative to past natural variability. It is the composite of ten individual climatic entities which have direct or indirect connection with climate dynamics. The aim to formalize the GCI is to provide a quantitative measurement of climate change. This index has showed the strongest expected climate change variability at global level and has measured the degree of variation by which climate is changing. It also illustrates natural climate variability and revealing how difficult it is to reliably perceive a change of quantities that are naturally chaotic.

The scientific sense of GCI is such that positive changes are expected with global warming whereas negative values would associate with cooling. Thus the index is intended to be a measure of whether and the climate change, but also to examine whether there is practically a signif-

icant change of the nature predicted for global warming. In this study we have found that, the strongest warming about 331.57 %, has been occurred by the end of 2018, relative to late 1970's due to anthropogenic factors only. Hence the anthropogenic factors are solely responsible for the present global warming and climate change. On the other hand the natural factors of climate system are responsible for climate variability only. This concludes that the Earth's climate is approaching towards further warming. Our proposed global climate index (GCI) is strongly correlated with global surface temperature, which has increased the reliability of our proxy climate index.

Acknowledgement

AB is thankful to University Grants Commission (UGC), India for proving partial financial support (National Fellowship). Authors are thankful to all data providers.

References

- [1] L. M. Andreassen, H. Elvehøy, B. Kjølmoen, R. V. Engeset, N. Haakensen. Glacier mass-balance and length variation in Norway. *Ann. Glaciol.*, 2005, 42: 317-325.
DOI: <https://doi.org/10.3189/172756405781812826>
- [2] M. N. Efstathiou, C. A. Varotsos. Intrinsic properties of Sahel precipitation anomalies and rainfall. *Appl. Climatol.*, 2012, 109: 627-633.
DOI: <https://doi.org/10.1007/s00704-012-0605-2>
- [3] IPCC. *Managing the Risks of Extreme Events and Disasters to Advance Climate Change Adaptation*, Cambridge University Press, Cambridge, UK, 2012: 555.
- [4] K. C. Busch, J. A. Henderson, K. T. Stevenson. *Broadening Epistemologies and Methodologies in Climate Change Education Research*. Environmental Education Research, 2018 25: 955-971.
DOI: <https://doi.org/10.1080/13504622.2018.1514588>
- [5] M. N. Efstathiou, C. A. Varotsos. On the 11 year solar cycle signature in global total ozone dynamics. *Meteorol. Appl.*, 2013, 20: 72-79.
DOI: <https://doi.org/10.1002/met.1287>
- [6] R. Blackport, P. Kushner. The Transient and Equilibrium Climate Response to Rapid Summertime Sea Ice Loss in CCSM4. *J. Clim.*, 2016, 29: 401-417.
DOI: <https://doi.org/10.1175/JCLI-D-15-0284.1>
- [7] D. Burçkin, A. Umut, Y. Özdem-Yılmaz, N. Öztürk, D. Sönmez. A model for pre-service teachers' climate change awareness and willingness to act for pro-climate change friendly behavior: adaptation of awareness to climate change questionnaire. *Int. Res.*

- Geograph. Env. Edu., 2015, 24: 184-200.
- [8] D. Notz, J. Stroeve. Observed Arctic sea-ice loss directly follows anthropogenic CO₂ emission. *Science*, 2016, 354: 747-750.
- [9] J. M. Arblaster, G. A. Meehl, D. J. Karoly. Future climate change in the Southern Hemisphere: Competing effects of ozone and greenhouse gases. *Geophys. Res. Lett.*, 2011, 38: L02701.
DOI: <https://doi.org/10.1029/2010GL045384>
- [10] J. E. Walsh. Intensified warming of the Arctic: Causes and impacts on middle latitudes. *Glob. Planet. Chang.*, 2014, 117: 52-63.
DOI: <https://doi.org/10.1016/j.gloplacha.2014.03.003>
- [11] R. O. Weber, P. Talkner. Spectra and correlations of climate data from days to decades. *J. Geophys. Res.*, 2001, 106: 20131-20144.
DOI: <https://doi.org/10.1029/2001JD000548>
- [12] Y. Xia, Y., Huang, Y., Hu. On the Climate Impacts of Upper Tropospheric and Lower Stratospheric Ozone. *J. Geophys. Res. Atmos.*, 2018, 123: 730-739.
DOI: <https://doi.org/10.1002/2017JD027398>
- [13] J. Lean, D. Rind. Evaluating sun-climate relationships since the Little Ice Age. *J. Atmos. Sol. Terr. Phys.*, 1999, 61: 25-36.
DOI: [https://doi.org/10.1016/S1364-6826\(98\)00113-8](https://doi.org/10.1016/S1364-6826(98)00113-8)
- [14] A. Bhargawa, A. K. Singh. Prediction of declining solar activity trends during solar cycles 25 and 26 and indication of other solar minimum. *Adv. Spa. Res.*, 2019, 64: 271-277.
DOI: <https://doi.org/10.1007/s10509-019-3500-9>
- [15] C. E. Iles, G. C. Hegerl. The global precipitation response to volcanic eruptions in the CMIP5 models. *Environ. Res. Lett.*, 2014, 09: 104012.
DOI: <https://doi.org/10.1088/1748-9326/9/10/104012>
- [16] S. Driscoll, A. Bozzo, L. J. Gray, A. Robock, G. Stenchikov. Coupled Model Intercomparison Project 5 (CMIP5) simulations of climate following volcanic eruptions. *J. Geophys. Res.*, 2012, 117: D17105.
DOI: <https://doi.org/10.1029/2012JD017607>
- [17] C. L. Parkinson, D. J. Cavalieri. Antarctic sea ice variability and trends, 1979-2010. *Cryosphere*, 2012, 06: 871-880.
DOI: <https://doi.org/10.5194/tc-6-871-2012>
- [18] T. Vihma. Effects of Arctic Sea Ice Decline on Weather and Climate: A Review. *Surv. Geophys.*, 2014, 35: 1175-1214.
DOI: <https://doi.org/10.1007/s10712-014-9284-0>
- [19] T. P. Hughes, A. H. Baird, D. R. Bellwood, et al., Climate Change, Human Impacts, and the Resilience of Coral Reefs. *Science*, 2003, 301: 929-933.
DOI: <https://doi.org/10.1126/science.1085046>
- [20] M. Ringnér. What is principal component analysis. *Nature Biotechnology*, 2008, 26: 303-304.
DOI: <https://doi.org/10.1038/nbt0308-303>
- [21] I. T. Jolliffe. *Principal Component Analysis*. Springer, New York, 2002.
- [22] R. W. Preisendorfer, C. D. Mobley. *Principal component analysis in meteorology and oceanography*, Elsevier, Amsterdam, 1988.
- [23] IPCC, Chapter 3: Impacts of 1.5°C global warming on natural and human systems. In: *Global Warming of 1.5 °C. Special Report of the Intergovernmental Panel on Climate Change*, 2018.
- [24] W. Herschel. Observation tending to investigate the nature of the sun. *Philos. Trans. R. Soc.*, 1801, 01: 265-318.
- [25] D. V. Hoyt, K. H. Schatten. *The Role of the Sun in Climate Change*. Oxford University Press, Oxford, 1997.
- [26] D. L. Damian, Y. J. Matthews, T. A. Phan, G. M. Halliday. An action spectrum for ultraviolet radiation - induced immunosuppression in humans. *Brit. J. Dermatol.*, 2011, 164: 657-659.
DOI: <https://doi.org/10.1111/j.1365-2133.2010.10161.x>
- [27] J. D. Haigh. The Impact of Solar Variability on Climate. *Science*, 1996, 272: 981-984.
DOI: <https://doi.org/10.1126/science.272.5264.981>
- [28] A. Bhargawa, M. Yakub, A. K. Singh. Repercussions of solar high energy protons on ozone layer during super storms. *Res. Astron. Astrophys.*, 2019, 19: 02.
DOI: <https://doi.org/10.1088/1674-4527/19/1/2>
- [29] J. M. Wilcox. Solar activity and the weather. *J. Atmospheric Sol. Terr. Phys.*, 1975, 37: 237-256.
DOI: [https://doi.org/10.1016/0021-9169\(75\)90108-7](https://doi.org/10.1016/0021-9169(75)90108-7)
- [30] R. E. Dickinson. solar variability and the lower atmosphere. *Bull. Am. Meteorol. Soc.*, 1975, 56: 1240-1248.
DOI: [https://doi.org/10.1175/1520-0477\(1975\)056<1240:SVATLA>2.0.CO;2](https://doi.org/10.1175/1520-0477(1975)056<1240:SVATLA>2.0.CO;2)
- [31] R. Markson, M. Muir. Solar Wind Control of the Earth's Electric Field. *Science*, 1980, 206: 979.
DOI: <https://doi.org/10.1126/science.208.4447.979>
- [32] B. W. Tinsley, G. W. Deen. Apparent tropospheric response to MeV - GeV particle flux variations: A connection via electrofreezing of supercooled water in high - level clouds? *J. Geophys. Res.*, 1991, 96: 22283-22296.
DOI: <https://doi.org/10.1029/91JD02473>
- [33] E. Bard, M. Frank. Climate change and solar variability: What's new under the sun? *Earth Planetary Sci. Lett.*, 2006, 248: 01-14.
DOI: <https://doi.org/10.1016/j.epsl.2006.06.016>
- [34] C. D. Camp, K. K. Tung. Surface warming by the

- solar cycle as revealed by the composite mean difference projection. *Geophys. Res. Lett.*, 2007, 34: L14703.
DOI: <https://doi.org/10.1029/2007GL030207>
- [35] S. Madronich, R. L. McKenzie, L. O. Björn, M. M. Caldwell. Changes in biologically active ultraviolet radiation reaching the Earth's surface. *J. Photochem. Photobiol. B.*, 1998, 46: 05-19.
DOI: [https://doi.org/10.1016/S1011-1344\(98\)00182-1](https://doi.org/10.1016/S1011-1344(98)00182-1)
- [36] A. K. Singh, A. Bhargawa. Atmospheric burden of ozone depleting substances (ODSs) and forecasting ozone layer recovery. *Atmospheric Pollution. Research*, 2019, 10: 802-807.
DOI: <https://doi.org/10.1016/j.apr.2018.12.008>
- [37] P. Gies, C. Roy, J. Javorniczky, S. Henderson, L. Lemus-Deschamps, C. Driscoll. Global Solar UV Index: Australian Measurements, Forecasts and Comparison with the UK. *Photochem. Photobiol.*, 2004, 79: 32-39.
DOI: <https://doi.org/10.1111/j.1751-1097.2004.tb09854.x>
- [38] S. M. Kang, L. M. Polvani, J. C. Fyfe, M. Sigmond. Impact of Polar Ozone Depletion on Subtropical Precipitation. *Science*, 2011, 332: 951-954.
DOI: <https://doi.org/10.1126/science.1202131>
- [39] J. T. Kiehl. On the Observed Near Cancellation between Longwave and Shortwave Cloud Forcing in Tropical Regions. *J. Clim.*, 1994, 07: 559-565.
DOI: [https://doi.org/10.1175/1520-0442\(1994\)007<0559:OTONCB>2.0.CO;2](https://doi.org/10.1175/1520-0442(1994)007<0559:OTONCB>2.0.CO;2)
- [40] D. L. Hartmann, L. A. Moy, Q. Fu. Tropical Convection and the Energy Balance at the Top of the Atmosphere. *J. Clim.*, 2001, 14: 4495-4511.
DOI: [https://doi.org/10.1175/1520-0442\(2001\)014<4495:TCATEB>2.0.CO;2](https://doi.org/10.1175/1520-0442(2001)014<4495:TCATEB>2.0.CO;2)
- [41] J. Herman, M. T. DeLand, L. K. Huang, G. Labow, D. Larko, et al. A net decrease in the Earth's cloud, aerosol, and surface 340 nm reflectivity during the past 33 yr (1979-2011). *Atmospheric Chem. Phys.*, 2012, 13: 8505-8524.
DOI: <https://doi.org/10.5194/acp-13-8505-2013>
- [42] R. Eastman, S. G. Warren, C. J. Hahn. A 39-Yr Survey of Cloud Changes from Land Stations Worldwide 1971-2009: Long-Term Trends, Relation to Aerosols, and Expansion of the Tropical Belt. *J. Clim.*, 2013, 26: 1286-1303.
DOI: <https://doi.org/10.1175/JCLI-D-12-00280.1>
- [43] P. R. Goode, E. Pallé. Shortwave forcing of the Earth's climate: Modern and historical variations in the Sun's irradiance and the Earth's reflectance. *J. Atmospheric Sol. Terr. Phys.*, 2007, 69: 1556-1568.
DOI: <https://doi.org/10.1016/j.jastp.2007.06.011>
- [44] A. A. Lacis, G. A. Schmidt, D. Rind, R.A. Ruedy. Atmospheric CO₂: Principal Control Knob Governing Earth's Temperature. *Science*, 2010, 330: 356-359.
DOI: <https://doi.org/10.1126/science.1190653>
- [45] M. Collins, S. I. An, W. Cai, A. Ganachaud, et al., The impact of global warming on the tropical Pacific Ocean and El Niño. *Nat. Geosci.*, 2010, 3: 391-397.
DOI: <https://doi.org/10.1038/ngeo868>
- [46] W. Cai, A. Santoso, G. Wang, S. W. Yeh, S. I. An, K. M. Cobb, et al., ENSO and greenhouse warming. *Nat. Clim. Chan.*, 2015, 5: 849-859.
DOI: <https://doi.org/10.1038/nclimate2743>
- [47] C. T. Y. Chung, S. B. Power, J. M. Arblaster, H. A. Rashid, G. L. Roff. Nonlinear precipitation response to El Niño and global warming in the Indo-Pacific. *Clim. Dynam.*, 2014, 42: 1837-1856.
DOI: <https://doi.org/10.1007/s00382-013-1892-8>
- [48] IPCC, Impacts, Adaptation, and Vulnerability. Part A: Global and Sectoral Aspects, the Fifth Assessment Report of the Intergovernmental Panel on Climate Change, 2014.
- [49] R. Batehup, S. McGregor, A. J. E. Gallant. The influence of non-stationary teleconnections on palaeoclimate reconstructions of ENSO variance using a pseudoproxy framework. *Climate of the Past*, 2015, 11: 1733.
DOI: <https://doi.org/10.5194/cp-11-1733-2015>
- [50] E. A. Barnes, S. Solomon, L. M. Polvani. Robust Wind and Precipitation Responses to the Mount Pinatubo Eruption, as Simulated in the CMIP5 Models. *J. Climate*, 29: 4763-4778.
DOI: <https://doi.org/10.1175/JCLI-D-15-0658.1>
- [51] N. P. Gillett, A. J. Weaver, F. W. Zwiers, M. F. Wehner. Detection of volcanic influence on global precipitation. *Geophys. Res. Lett.*, 2004, 31: L12217.
DOI: <https://doi.org/10.1029/2004GL020044>
- [52] F. Liu, J. Chai, B. Wang, J. Liu, et al. Global monsoon precipitation responses to large volcanic eruptions. *Sci. Rep.*, 2016, 6: 24331.
DOI: <https://doi.org/10.1038/srep24331>
- [53] J. Hansen, M. Sato, R. Ruedy, K. Lo, D. W. Lea. Global temperature change. *Proc. Natl. Acad. Sci. USA*, 2006, 03: 14288-14293.
DOI: <https://doi.org/10.1073/pnas.0606291103>
- [54] A. Dai, J. Fyfe, S. Xie, et al., Decadal modulation of global surface temperature by internal climate variability. *Nature Clim. Change*, 2015, 5: 555-559.
DOI: <https://doi.org/10.1038/nclimate2605>
- [55] X. Yun, B. Huang, J. Cheng, et al. A new merge of global surface temperature datasets since the start of the 20th century. *Earth Syst. Sci. Data*, 2019, 11: 1629-1643.

- DOI: <https://doi.org/10.5194/essd-11-1629-2019>**
- [56] J. A. Church, J. M. Gregory, P. Huybrechts, et al. Climate Change: The Scientific Basis: Contribution of Working Group I to the Third Assessment Report of the Intergovernmental Panel, 2001.
- [57] J. A. Church, N. J. White. Sea-Level Rise from the Late 19th to the Early 21st Century. *Surv. Geophys.*, 2011, 32: 04-16.
DOI: <https://doi.org/10.1007/s10712-011-9119-1>
- [58] C. L. Parkinson, D. J. Cavalieri, P. Gloersen, et al., Arctic sea ice extents, areas, and trends, 1978-1996. *J. Geophys. Res.*, 1999, 104: 20837-20856.
DOI: <https://doi.org/10.1029/1999JC900082>
- [59] R. Kwok, D. A. Rothrock. Decline in Arctic sea ice thickness from submarine and ICESat records: 1958-2008. *Geophys. Res. Lett.*, 2009, 36: L15501.
DOI: <https://doi.org/10.1029/2009GL039035>
- [60] J. C. Stroeve, M. C. Serreze, M. M. Holland, et al., The Arctic's rapidly shrinking sea ice cover: a research synthesis. *Clima. Change*, 2012, 110: 1005-1027.
DOI: <https://doi.org/10.1007/s10584-011-0101-1>
- [61] J. A. Screen, I. Simmonds, C. Deser, R. Tomas. The Atmospheric Response to Three Decades of Observed Arctic Sea Ice Loss. *J. Climate*, 2013, 26: 1230-1248.
DOI: <https://doi.org/10.1175/JCLI-D-12-00063.1>
- [62] H. J. Zwally, J. C. Comiso, C. L. Parkinson, et al., Variability of Antarctic sea ice 1979-1998. *J. Geophys. Res.*, 2002, 107: 3041.
DOI: <https://doi.org/10.1029/2000JC000733>
- [63] J. Turner, J. S. Hosking, T. Phillips, G. J. Marshall. Temporal and spatial evolution of the Antarctic sea ice prior to the September 2012 record maximum extent. *Geophys. Res. Lett.*, 2013, 40: 5894-5898.
DOI: <https://doi.org/10.1002/2013GL058371>
- [64] J. E. Walsh. MELTING ICE: What Is Happening to Arctic Sea Ice, and What Does It Mean for Us? *Oceanography*, 2013, 26: 171-181.
- [65] W. S. Zhang, S. Lin, X. M. Jiang. Influences of natural variability and anthropogenic forcing on the extreme 2015 accumulated cyclone energy in the Western North Pacific. *Bull. Amer. Meteor. Soc.*, 2016, 97: S131-S135.